Band structure effects in the conductivity of graphite in a strong magnetic field. Alfven waves

G. A. Kapustin, V. S. Babichenko, and E. Z. Meilikhov

I. M. Kurchatov Atomic Energy Institute

(Submitted 9 March 1988)
Zh. Eksp. Teor. Fiz. **94**, 330–345 (September 1988)

We have measured the high-frequency conductivity of graphite in magnetic fields up to 200 kOe for $T = 4.2$ K by studying the propagation of Alfven waves ($\lambda = 2$ and 4 mm, $\mathbf{q} \| \mathbf{H} \| \mathbf{c}$, where $\mathbf{c}$ is the hexagonal axis of graphite) in samples of kish-graphite. It is shown that the propagation of Alfven waves at sufficiently high frequencies is accompanied by beats of the signals from electron- and hole-active waves. We propose a simple model for the HF conductivity of graphite in the regions of classical strong and weakly quantizing magnetic fields, with account taken of contributions to the conductivity from intraband and interband electron transitions; this model provides a good description of the experimentally observed beat pattern. We obtain the magnetic-field dependences of the carrier mass densities and the frequencies which characterize their momentum-relaxation rates, and show that these dependences are qualitatively different for $H \gtrsim 20$ kOe and $H \lesssim 20$ kOe. By comparing results of HF measurements with those of galvanomagnetic measurements [Brand and Kapustin, Sov. Phys. JETP **40**, 564 (1975)] we have established that peculiarities obtained in the latter in the field dependence of the transverse magnetoresistivity of graphite in quantizing fields and in the ultraquantum limit are due to peculiarities in the band structure of graphite, particularly to the rapid growth in the carrier mass density for $H \gtrsim 20$ kOe. We determine the value of the band structure parameter γ_6 of graphite for two samples ($\gamma_6 = 36 \pm 7$ and -55 ± 7 meV).

INTRODUCTION

The investigation of galvanomagnetic (GM) properties of various forms of graphite (native single-crystal, pyrolytic and kish-graphite) in fairly perfect crystal structures has been a topic of a large number of papers.[1–20] As a rule, interpretations of the results are formulated using the single-electron band structure model proposed by Slonczewski and Weiss[21] (the SW model), which is specified by six parameters γ_i ($i = 1,...,6$), five of which ($i = 1,...,5$) include the interactions of atoms from different layers of the lattice. In the absence of interlayer interactions, graphite would be a two-dimensional zero-gap semiconductor; in reality it is a semimetal (the band overlap is $\approx$35–40 meV) with almost identical concentrations of electrons and holes ($n_e = n_h \approx 2 \times 10^{18}$ cm^{-3} for $T \to 0$ and $B = 0$), whose masses (in the basal plane) are $m_e = 0.057\ m_0$, $m_h = 0.039 m_0$.

The SW model gives a good description of the GM properties of graphite in classically strong magnetic fields, and also of the Shubnikov–de Haas (SdH) oscillations in a quantizing field. However, numerous attempts to interpret the general forms of the field and temperature dependences of the resistivity ρ_{xx} in a quantizing field (especially in the region of the ultraquantum limit) have ended in failure. The essential complexity of the problem lies in the necessity of separating the calculation of the band-structure singularities from that of carrier scattering; information about the latter is impossible to obtain if we study only the GM properties of the semimetal, where $n_e \approx n_h$. Therefore it was customary to use crude model representations of the carrier scattering mechanisms, which have led to obvious contradictions with experiments.

In this situation, all problems would be resolved if we could carry out experiments which would permit us to obtain independent information about the roles of band structure and carrier scattering in determining the GM properties of graphite. One such experiment would be to measure the HF conductivity $\sigma^{\omega}_{\alpha\beta}$ ($\alpha,\beta = x,y$) of graphite in a magnetic field; if the cyclotron frequency $\omega_{cj} \gg \nu_j$ and the frequency ν_j which characterizes the momentum relaxation rate of the jth carrier type ($j = e,h$) are such that $\omega_{cj} \gg \nu_j$, (where ω is the frequency of the electromagnetic field), then $\mathrm{Re}\ \sigma^{\omega}_{xx} = \sigma^{0}_{xx}$ (under the condition that ν_3 does not depend on ω), while $\mathrm{Im}\ \sigma^{\omega}_{xx}$ is determined only by the band structure. Therefore separate measurements of $\mathrm{Re}\ \sigma^{\omega}_{xx}$ and $\mathrm{Im}\ \sigma^{\omega}_{xx}$ would allow us to isolate the band-structure contributions to the conductivity. Such measurements can be carried out by studying the propagation of Alfven waves (AW) with wave vectors $\mathbf{q} \| \mathbf{H} \| \mathbf{c} \| \mathbf{z}$ (where $\mathbf{c}$ is the hexagonal axis).

Although investigations of the propagation of AW in graphite have been carried out previously (Refs. 22–25), the results of GM and HF measurements reported in these papers are not comparable—in fact, they are mutually contradictory. In our paper, we pursue twin goals: (1) to clarify the causes of the disagreement between these previous HF and GM measurements of the conductivity of graphite, and (2) to separate the band-structure contributions to the peculiarities of the graphite conductivity from those of carrier scattering, by carrying out HF measurements over a wide range of magnetic fields.

1. KINETIC PROPERTIES OF GRAPHITE IN A MAGNETIC FIELD

1.1. Galvanomagnetic properties

The high mobility of carriers in the basal plane of graphite (which can rise to $\sim 10^6$ cm^2/V·sec at $T = 4.2$ K) and near-total carrier compensation ($|\Delta n|$

 0038-5646/88/091922-09$04.00

$= |n_e - n_h| \lesssim 0.1 n_e$) leads at helium temperatures to carrier magnetization (for $\mathbf{H}\|\mathbf{c}$) and a rapid growth of resistance even in fields $H \sim 10$–100 Oe. However, the relation $\rho_{xx} \propto H^2$ typical of simple models of a semimetal, in which it is assumed that $n_j, \nu_j = \text{const}$, is not observed in either native[2] or artificial[1,3–8] graphite.

The quantization of the spectrum becomes significant even in fields $H \sim 10^3$–10^4 Oe, while for $H > H_{\text{UQL}} \approx 70$ kOe the ultraquantum limit (UQL) is reached. The associated oscillatory phenomena[8–12] agree with the SW model[26]; however, they are observed against a background component of $\rho_{xx}(H)$ which is large and which increases monotonically in an approximately linear manner with field. This linearity is preserved even in the UQL (up to 160 kOe for $T = 4.2$ K; see Ref. 13). In large fields $\rho_{xx}(H)$ saturates, an effect which is more marked at 77 K (Ref. 1). However, the product $\sigma_{xx} H \propto \Delta n$ remains constant only for $H \lesssim 200$ kOe, while in large fields $|\Delta n|$ decreases sharply; this effect has been associated with magnetic freezeout of the carriers.[1] Saturation of $\rho_{xx}(H)$ is observed both in native[15–17] and in artificial[15–18] graphite.

For $H \lesssim 10$–20 kOe the function $\rho_{xx}(T)$ decreases monotonically with increasing temperature, while for large fields (including the UQL) $\rho_{xx}(T)$ passes through a maximum at $T = 20$–30 K (Refs. 16 and 17). Thus, a change occurs in the character of the field and temperature dependences of ρ_{xx} in graphite for fields $H \sim 20$ kOe.

Up until now an adequate explanation has not been advanced for any of the following anomalies: the nonquadratic dependence of ρ_{xx} in a quantizing field, the saturation of ρ_{xx} in the UQL, and the temperature dependence of ρ_{xx}. The authors of Ref. 13 claimed that the linear dependence of $\rho_{xx}(H)$ in the UQL was connected with carrier scattering by charged impurities whose screening radius decreases with field. However, this model does not explain the saturation of $\rho_{xx}(H)$. In Ref. 1 it was assumed that the latter is related to an increasing carrier concentration in the UQL. However, the calculations in Ref. 27 showed that for $30 \text{ kOe} \lesssim H \lesssim 400$ kOe this increase is linear in the field, and consequently cannot be the cause of the eventual saturation of $\rho_{xx}(H)$. In Ref. 17 the saturation of $\rho_{xx}(H)$ was explained by invoking a transition from carrier scattering by charged impurities to scattering by neutral impurities, which occurs as a result of magnetic freezeout of impurity carriers. However, the saturation of $\rho_{xx}(H)$ takes place even for samples (and temperatures) in which magnetic freezeout was not observed. Thus, none of the hypotheses listed above can explain the changeover from a linearly-increasing to a saturating $\rho_{xx}(H)$.

We note that researchers have recently observed sharp changes in the function $\rho_{xx}(H)$ in a number of graphite samples at $T \lesssim 4.2$ K in fields ~ 300–400 kOe, which were interpreted as a phase transition in the electronic system accompanied by formation of charge density waves (see, e.g., Refs. 19 and 20).

1.2. Alfven waves in graphite

We can find the complex HF conductivity σ_{xx}^{ω} of graphite by studying the propagation in it of electromagnetic waves. For nearly equal concentrations of electrons and holes ($|\Delta n| \ll n_c$), AW are weakly damped (for $\omega \gg \nu_j$) and propagate along $\mathbf{H}\|z$ with the dispersion law

$$q^2 c^2/\omega^2 = \varepsilon_L + i(4\pi/\omega)\sigma_{xx}^{\omega}, \tag{1}$$

where ε_L is the permittivity of the lattice. In a classical strong magnetic field which satisfies the condition

$$\omega_{cj} \gg |\omega - i\nu_j| \gg q v_j^F \tag{2}$$

(where v_j^F is the Fermi velocity of the carriers), we have

$$\sigma_{xx}^{\omega} = D(c^2/H^2)(\bar{\nu} - i\omega), \tag{3}$$

where

$$D = \sum_j n_j m_j, \qquad \bar{\nu} = \frac{1}{D}\sum_j n_j m_j \nu_j,$$

and D is the carrier mass density.

By measuring the real (q_r) and imaginary (q_i) parts of q, we can find σ_{xx}^{ω} with the help of (1). A popular method of investigating the propagation of electromagnetic waves is the interferometric method, based on the mixing of a wave passing through the sample (a plane parallel film of thickness l) with a reference wave (i.e., a Rayleigh interferometer). If $q_r l \gg q_i l \gg 1$, the complex transmission coefficient β (the ratio of the transmitted and incident field amplitudes of circularly-polarized waves) for normal incidence equals[28]:

$$\begin{aligned} &\beta = |t| e^{-\alpha} e^{iq_r l}, \\ &\alpha = q_i l, \quad |t| = 4q_r(\omega/c)(\omega/c + q_r)^{-2}. \end{aligned} \tag{4}$$

Mixing of the transmitted (of amplitude $|\beta|E_0$) and incident (of amplitude $E_{\text{ref}} \gg |\beta| E_0$) waves in a detector gives a signal which oscillates with the magnetic field. The position and amplitude A of the extrema are determined by the relations

$$q_r l + \varphi = M\pi, \quad A = A_0 |t| e^{-\alpha}, \tag{5}$$

where φ is the phase difference between the incident and reference waves, M is an integer which labels a particular extremum, and $A_0 \propto E_{\text{ref}} E_0$ is the amplitude of the signal in the absence of a sample. Knowing the functions $M(H)$ and $\alpha(H)$, we can obtain the functions $q_r(H)$ and $q_i(H)$ from (5), and then with the help of (1) we can find σ_{xx}^{ω}. In particular, it follows from (1) and (3) that in that region of fields where D and $\bar{\nu}$ do not depend on H, and ε_L can be neglected, plots of the functions $M(1/H)$ and $\alpha(H)$ are straight lines whose slopes determinee D and $\bar{\nu}$.

A similar method was used in previous studies of the propagation of AW in graphite,[22–25] dealing not so much with the physical properties of these waves as with the peculiarities of their propagation in an anisotropic medium such as graphite. The physical results were based on the assumption that D and $\bar{\nu}$ did not depend on H. With this assumption it is found that $\rho_{xx} \approx H^2/c^2 D\bar{\nu} \propto H^2$; this clearly contradicts the results of the GM measurements. However, comparison of the HF and GM measurements was not carried out in these papers.

As our experiments have shown,[29,30] D and $\bar{\nu}$ depend substantially on H. These functions are qualitatively different; for $H \lesssim 20$ kOe we have $D = \text{const}$ and $\bar{\nu} \propto H$, whereas for $H \gtrsim 20$ kOe we find that $\bar{\nu} \approx \text{const}$ while D grows linearly with field (for $H \gtrsim 60$ kOe this growth is superlinear). Thus, the results of Refs. 22–25 require reexamination. A superlinear $D(H)$ dependence for $H \gtrsim 50$ kOe was also observed in Ref. 31. However, the function described in Ref. 31 lies con-

siderably above the curve obtained in this paper. In what follows we will discuss this disagreement.

2. MEASUREMENT METHOD

Our measurements were carried out with a Rayleigh interferometer at $T = 4.2$ K in the two- and four-millimeter bands for a magnetic field orientation $\mathbf{H}\|\mathbf{c}\|\mathbf{q}\perp\mathbf{E}$, using a linearly-polarized incident wave and linear or elliptically-polarized reference waves in stationary (up to 88 kOe) and pulsed (up to 200 kOe with a half-period 8 msec) magnetic fields, on samples of kish-graphite analogous to those investigated in Ref. 1. The sample thicknesses in mm were: 0.123 (KG-1), 0.165 (KG-2), and 0.020 (KG-3). In addition, we studied the dependence of the wave power transmitted through the sample on H in the stationary fields.

Waveguide channels (Fig. 1) using mainly 7.2×3.4 mm waveguides, allowed us to work with both linear and elliptically-polarized reference waves. The sample was glued to the narrow end of a waveguide junction (with cross-section 2×1 mm^2 for $\lambda\approx2$ mm, and 3×1.5 mm^2 for $\lambda\approx4$ mm); this junction was used to "cut off" the higher waveguide modes and to ensure linear polarization of the incident wave. We used a delay line to equalize the lengths of the interferometer arms during measurements in stationary magnetic fields. The drift in the phase difference of waves in the arms of the interferometers did not exceed 5° over 8 hours.

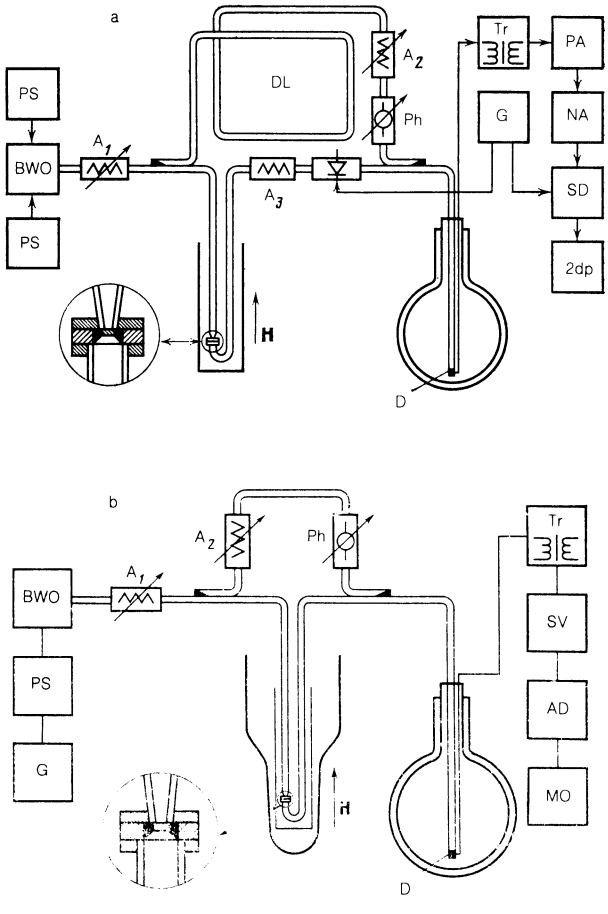

FIG. 1. Block diagrams of the measurement portions of the setup for investigating the propagation of Alfven waves in graphite in stationary (a) and pulsed (b) fields: BWO—backward-wave oscillator tube; PS—SVL-341 power supply; CS—current stabilizer for the BWO tube filament; A_1–A_3—attenuators; DL—delay line; Ph—phase shifter; D—InSb detector; TR—matching transformer; PA—preamplifier; NA—narrow-band amplifiers U_2–U_6; SD—K3-2 lock-in detector; 2DP—PDP-4-002 x-y plotter; SV—B6-1 selective microvoltmeter; AD—pulse-height detector; MO—C8-11 memory oscilloscope; G—G100-I modulating-voltage generator.

A special difficulty related to the large attenuation of the waves in the sample (the ratio of the incident to transmitted wave powers can be as large as 10^8) is the elimination of the microwave signal which leaks past the sample and through joints between sections of the waveguide circuit. Owing to our use of a paste of powdered technically pure graphite and AGO glue for gluing the sample and "sealing" the joints, in our stationary-field investigations the parasitic millimeter-wave signal levels were below the detection capability of the detector at $H = 0$. For the pulsed magnetic field studies the parasitic signal amounted to 10% of the useful signal ($H \lesssim 20$ kOe); however, the appearance of this parasitic signal was related to the presence of discontinuities (for eliminating eddy currents) in the waveguides and does not lead to parasitic modulation of the amplitude and phase of the signal as H is varied.

We used a cooled (to $T = 4.2$ K) photoelectric cell made from n-InSb with a sensitivity of 370 V/W (at $\lambda = 8$ mm) as a detector. The deviation of the IV curve from linearity did not exceed 1 dB at an incident power level of $2\cdot10^{-5}$ W.

The high sensitivity of this detector, which in stationary fields amounted to $\approx3\cdot10^{-12}$ W GHz$^{-1/2}$ with the receiver apparatus connected, is a consequence of modulation of the millimeter-wave signal power with increased frequency ($f_{\text{mod}} = 12$ and 175 kHz for stationary and pulsed fields, respectively) and the subsequent extraction of the detector signal from the frequency-modulated signal using a narrow-band amplifier; the latter was matched to the detector by using low-noise resonant transformers. Modulation of the millimeter-wave signal for measurements made in pulsed fields was accomplished by varying the voltage at the anode of the backward-wave oscillator (BWO) tube, while for the stationary-field measurements this was done using a modulator made of two KA513B pin-diodes. In the latter case the spectra density of the receiver noise came to 0.2 nW GHz$^{-1/2}$ ($f = 12$ GHz), which is twice as low as the noise level of the InSb detector (together with the receiver apparatus).

The stationary magnetic field was measured to better than 1% accuracy, and was calibrated against the EPR signal in diphenyl picryl hydrazyl (DPPH). The pulsed magnetic field was calibrated against the ferromagnetic resonance signal in yttrium iron garnet; the error in the measurement was no worse than 3%. The error in measuring the amplitudes of the interference extrema is determined primarily by the instability of the BWO output power and amounts to 5–10%. The error in the absolute measurements of the wave attenuation in the sample was $\lesssim 3$ dB.

3. ALFVEN WAVES IN GRAPHITE

The scheme for measuring σ_{xx}^{ω} described in Sec. 1 has two features which were not included in previous papers[22–25]; their omission can lead not only to quantitative errors but also to qualitatively incorrect results.

First of all, determination of $q_r(H)$ and $q_i(H)$ from (4) and (5) requires knowledge of the absolute values of M and α, whereas these values usually are determined using

model representations of the dispersion law for carriers in the material under study. In particular, a simple model of a semimetal having two types of carrier with n_j, m_j, and $\nu_j = \text{const}$ was in fact used in Refs. 22–25. However, taken by itself, the linearity of the experimental functions $M(1/H)$ and $\alpha(M)$ in a narrow region of fields is insufficient to confirm the applicability of this model. Such confirmation requires direct proportionality between M and $1/H$, α and M, which is impossible to verify experimentally without calibration.[1)] Overlooking this circumstance, Refs. 22–25 led to qualitative discrepancies between the HF and GM measurements.

To avoid similar errors, in our experiments we performed (in the absence of a reference wave) the following calibration of the wave attenuation in the sample; placing the sample under study in one arm of the interferometer, we measured the microwave power passing through this arm (in a sufficiently strong magnetic field); we then removed the sample and measured the power again, and took the ratio of these two powers. We determined the absolute values of M from the $M(1/H)$ dependence in the region of weakly-quantizing magnetic fields ($H \lesssim 20$ kOe), using a model (see Sec. 4) of the HF conductivity of graphite based on the results of quantum-mechanical calculations of the conductivity.

Secondly, Eq. (2), or in the general case the conditions

$$|\operatorname{Re}\sigma_{xy}^{\omega}| \ll |\operatorname{Im}\sigma_{xx}^{\omega}|, \quad |\operatorname{Im}\sigma_{xy}^{\omega}| \ll |\operatorname{Re}\sigma_{xx}^{\omega}| \tag{6}$$

for the applicability of the dispersion relation (1) are sufficient only for circularly-polarized waves. For linear (or elliptical) polarization we must add the condition that the phase difference and attenuation of the electron- and hole-active waves[2)] over the sample length be small:

$$l|q_{re}-q_{rh}| \ll 1, \quad l|q_{ie}-q_{ih}| \ll 1. \tag{7}$$

If condition (7) is not satisfied, then a small change (over a wavelength) in the difference between the phases and attenuations of these waves leads to the appearance of a significant difference between the phases and amplitudes of the waves at the output end of the sample. In this case beats of two oscillating signals take place at the detector (as the magnetic field varies); each of these signals is the result of the superposition of two waves (the wave passing through the sample and the reference wave) with circular polarizations in the same direction.

In the presence of beats, the amplitudes of the interference extrema are not single-valued functions of M or magnetic field, but rather depend on the direction of the latter [along (H^+) or opposite to (H^-) the direction of wave propagation] and on the ratio of the amplitudes $p = E_{\text{ref}}^{r}/E_{\text{ref}}^{l}$ and the phase difference $\Delta\varphi = \varphi_r'' + \varphi_l''$ of the reference waves with right-hand (r) and left-hand (l) polarizations. In this case it is convenient to characterize the amplitudes of the extrema by an effective transmission coefficient β^* equal to the ratio of the envelopes of the signal from the detector in the presence and absence of the sample:

$$\beta^{*\pm} = \left\{ \frac{|\beta_h|^2 + |\beta_e|^2 p^{\pm 2} + 2p^{\pm 1}|\beta_e\beta_h|\cos[\Delta\varphi \pm (\theta_e - \theta_h)]}{1 + p^{\pm 2} + 2p^{\pm 1}\cos\Delta\varphi} \right\}^{1/2}. \tag{8}$$

Here β_j is the transmission coefficient of the circularly-polarized waves at normal incidence,[28] $\theta_j = q_{rj}l + \xi_{ij} + \xi_{2j}, \xi_{1j}, \xi_{2j}$ are additional phase shifts produced at the boundary of the sample (ξ_{1j}), or as a result of interference of the multiply-reflected waves within the sample (ξ_{2j}); the upper and lower signs refer to the directions H^+ and H^- of the magnetic field. In the presence of beats, the relation between $\bar{\nu}$ and $\alpha^* = \ln(|t|/\beta^*)$ becomes more complicated; however, even in this case the monotonic component of the function $\alpha^*(H)$ is determined primarily by the function $\bar{\nu}(H)$. In strong magnetic fields which satisfy condition (7), $|\beta_e| = |\beta_h|$; the transmission coefficients β^{*+} and β^{*-} are then equal and coincide with the transmission coefficient $\beta_w = [(|\beta_e|^2 + |\beta_h|^2)/2]^{1/2}$, which is determined by the ratio of the incident and transmitted microwave signal powers. It is this relation which allows us to calibrate the absolute magnitudes of the $\beta^{*\pm}$. The magnetic fields corresponding to extrema of the resulting interferogram are given by the conditions

$$(\theta_e - \theta_h)/2 + (\varphi^r + \varphi^l)/2 + \psi^{\pm} = M\pi, \quad M = 1, 2, \ldots,$$

$$\operatorname{tg}\psi^{\pm} = \frac{|\beta_e|p^{\pm 1} - |\beta_h|}{|\beta_e|p^{\pm 1} + |\beta_h|} \operatorname{tg}\left[\frac{\pm(\theta_e - \theta_h) + \Delta\varphi}{2}\right] \tag{9}$$

and are determined by the average (over the two directions of circular polarization) of the phase advance in the sample and the phase shift between the reference and incident waves. Exceptions are the magnetic-field regions near values satisfying the relation

$$\pm(\theta_e - \theta_h) + \Delta\varphi = \pi(2L+1), \quad L = 0, \pm 1, \pm 2, \ldots,$$

where the beats lead to the appearance of dips on the plots of the amplitudes of the extrema vs H and to jumps of $\pm\pi$ in the phase of the interference pattern.

In Fig. 2 we show typical interferograms. Note the nonmonotonic character of the field dependence of the amplitudes of their extrema, and the differences in amplitude and phase for the two directions of H at $H \lesssim 30$ kOe, when the $M(1/H)$ plots (Fig. 3) show phase jumps whose locations coincide with the minima of the interferogram envelope (Fig. 4).[3)] The number and position of these singularities, and also their character, are different for different samples and vary both with the frequency of the microwave signal and (for an elliptically-polarized reference wave) with the direction of **H**. This radically distinguishes such singularities from SdH oscillations, and allows us to identify them as a consequence of the beats of the electron- and hole-activated waves. The authors of Ref. 24 erroneously assumed that at close mobilities μ_j there will be no such beats. However, we cannot exclude the possibility that at least a part of the dips in the $\beta(H)$ plots (Ref. 24) in weak magnetic fields (below the range of fields in which SdH oscillations of the majority carriers occur) are due just to beats and not to SdH oscillations of the minority carriers, as assumed by the authors of Ref. 24.

The dispersion laws for electron- and hole-activated waves are different because of the following effects: (1) the resonance contribution made to the dispersion of the electron- and hole-activated waves by the interband transition $(0^h - 0^e)_c$ of electrons between the lowest ($N = 0$) Landau levels of the majority carriers near the conical point $k_z = k_{zc}$ (where k_z is the wave vector of electrons in the direction $c \| z$ of graphite), at which the Fermi surfaces of the majority

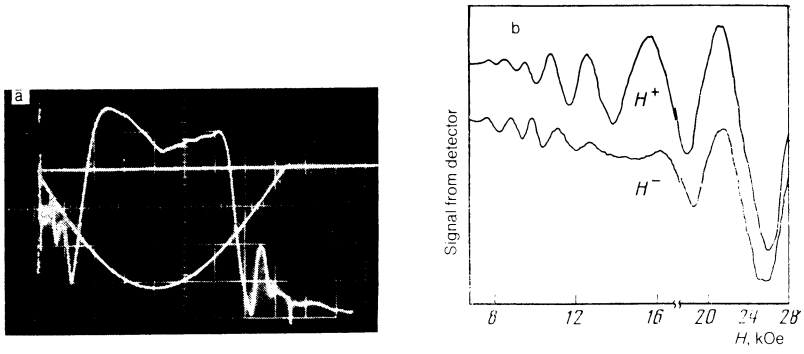

FIG. 2. Typical millimeter-wave interferograms at $T = 4.2$ K. The magnetic field was: (a) pulsed (smooth curve) with an amplitude of 196 kOe for sample KG-2, with $f = 131.73$ GHz; (b); stationary and directed along (H^+) and opposite to (H^-) the wave propagation; $\mathbf{q} \| \mathbf{H} \| \mathbf{c}$, sample KG-1, $f = 123.17$ GHz. In fields above 17 kOe the sensitivity of the measurement scheme and the sweep scale of the magnetic field were decreased by a factor of two.

carriers are in contact at $H = 0$; (2) the contributions from cyclotron resonance of the majority carriers. The resonance values of H for the transition $(0^h - 0^e)_c$ and the field dependence of the transition energy

$$\Delta E(H) = E_{e,0}(H, k_{zc}) - E_{h,0}(H, k_{zc})$$

($E_{e,0}$ and $E_{h,0}$ are the energies of the lowest Landau levels of the majority carriers) show (see Fig. 5) that the Landau levels 0^e and 0^h are degenerate for $H < H_d$ ($H_d = 2.5 \pm 1.5$ kOe for sample KG-1, $H_d = 4.5 \pm 1.5$ kOe for sample KG-2). This can be explained by the effect of trigonal warping of the equal-energy surfaces ($\gamma_3 \neq 0$), in agreement with the results of calculations[32] of the band structure of graphite in a magnetic field. According to Ref. 33, this trigonal warping introduces in the energies of the 0^e and 0^h levels corrections that are only weakly dependent (at least for $H \geqslant 20$ kOe) on H. According to Ref. 33, the practically linear dependence $\Delta E(H)$ is preserved with decreasing H down to H_d; this is the reason for the weak dependence of $\partial(\Delta E)/\partial H$ on γ_3. Therefore, starting with the known rate of growth of ΔE with field and assuming that for $H > H_d$ the derivative $\partial(\Delta E)/\partial H$ does not depend on γ_3, we can determine the parameter γ_6 of the SW model ($\gamma_6 = -36 \pm 7$ meV for sample KG-1 and $\gamma_6 = -55 \pm 7$ meV for sample KG-2). The sign of $\gamma_6 < 0$ agrees with the calculated[34] band-structure parameters γ_i, and indicates a possible transition of graphite to a zero-gap state in a field $\sim 10^6$ Oe.[27] The different values of γ_6 for the two samples (note that the relative accuracy of γ_6 is considerably higher than the absolute accuracy) suggests that the value of this parameter (and possibly of the other parameters γ_i of the SW model) can differ for different samples; this partially explains the large scatter in the values of γ_6 given by various authors.

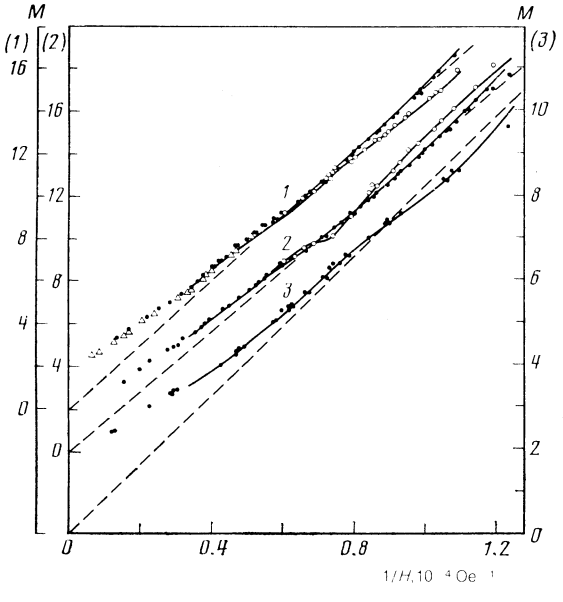

FIG. 3. Dependence of the number of extrema in the interference pattern on magnetic field for sample KG-1, $T = 4.2$ K. Points—experiment; solid curves—calculations using model (10) including beats; dashed lines—calculations using $D = \text{const}$ and without including heterodyning. Magnetic field: △—pulsed; ●, ○—stationary with direction along (●) and opposite (○) the wave propagation direction. Frequencies in GHz: *1*—131.90; *2*—123.17; *3*—71.50.

In Fig. 3 we show the functions $M(1/H)$ for sample KG-1 for different measurement frequencies. Each of these functions was obtained by joining several series of points corresponding to the positions of extrema on the interferograms which were taken for different values of the phase $(\varphi^l + \varphi^r)/2$ of the reference wave; in fact, M in (5) and (9) can even be noninteger. For $H \lesssim 20$ kOe the deviation of the experimental functions from the predicted $M \propto H^{-1}$ (i.e., the dashed lines with slopes corresponding to the mass density of the majority carriers) is not large, and is due primarily to beats of the electron- and hole-active waves, while for $H \gtrsim 20$ kOe the dependence of M on H for the samples studied here was considerably weaker than H^{-1}. The positions of the extrema were shifted to the high-field side, which indicates a rapid growth of the carrier mass density D with field. This conclusion qualitatively distinguishes the results of this paper from the earlier measurements,[23] according to which $D = \text{const}$ for $H \leqslant 140$ kOe.

In Fig. 4 we show the field dependences of the products $H \ln \beta^{*\pm}$ (interference measurements) and $H \ln \beta_w$ (transmitted signal-power measurements). For comparison, we show the dependence on H of the product $H \ln |t|$ (without taking into account the interference of the waves within the sample). In contrast to the results of Refs. 22–25, the monotonic component of the product $\alpha^* H$ (and consequently of $\bar{\nu}$ also) in the samples under study depends significantly on H; the character of the dependences differs for $H \lesssim 20$ kOe and $H \gtrsim 20$ kOe.

In the weak-magnetic-field region ($H \lesssim 10$ kOe for $\lambda \approx 2$ mm and $H \lesssim 5$ kOe for $\lambda \approx 4$ mm) the wave absorption in the sample and the number of extrema grow rapidly with

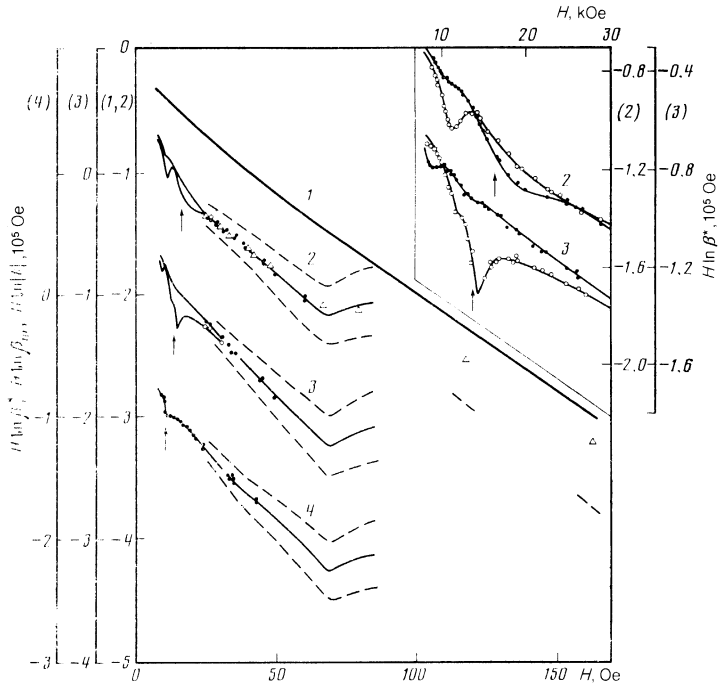

FIG. 4. Field dependence of the quantity $H \ln \beta^*$ (points: experiment), $H \ln \beta_w$ (solid curves for $H \geqslant 35$ kOe are from experiment) and $H \ln |t|$ (curve *1*, calculated) for sample KG-1 at $T = 4.2$ K. Shown with dashed lines are the limiting possible positions of the experimental curves, connected with the accuracy of calibration of the absolute value of the wave attenuation in the sample. The solid curves for $H \leqslant 30$ kOe were calculated according to the model (10) including beats. We note with arrows the fields which are resonant with the transition $(0^e - 0^h)_c$. Magnetic field: △—pulsed; ●, ○—stationary with direction along (●) and opposite (○) the propagation direction of the waves. Frequencies in GHz: *2*—131.90; *3*—123.17; *4*—71.50.

decreasing H; this is connected with the approach to the region of cyclotron resonance of the majority carriers.

4. PARAMETERS FOR THE CARRIER CURRENT

To interpret the complex picture of wave interference for $H \lesssim 20$ kOe, we used an HF-conductivity model based on the results of quantum mechanical calculations; this model takes into account contributions both from the majority carriers and from interband transitions. In this region of field, the former contribution is well-described by quasiclassical expressions with $n_j, m_j = \text{const}$, while the most important contribution from interband transitions is the resonance contribution from the transition $(0^h - 0^e)_c$. The latter can be represented in a form analogous to the contribution of the majority carriers, after which the expressions for σ_{xx}^{ω} take on the forms

$$\sigma_{xx}^{\omega} = \sum_{k=1}^{2} \frac{\omega_{ck}\left[\nu_k(\omega_{ck}^2+\omega^2+\nu_k^2) - i\omega(\omega_{ck}^2-\omega^2-\nu_k^2)\right]}{(\omega_{ck}^2-\omega^2+\nu_k)^2+(2\nu_k\omega)^2} \frac{n_k ec}{H},$$

$$\sigma_{xy}^{\omega} = \sum_{k=1}^{3} (-1)^k \left[\frac{\omega_{ck}^2(\omega_{ck}^2-\omega^2+\nu_k^2+2i\nu_k\omega)}{(\omega_{ck}^2-\omega^2+\nu_k)^2+(2\nu_k\omega)^2} - \delta_{k,3}\right] \frac{n_k ec}{H}. \quad (10)$$

Here the subscripts $k = 1,2$ refer to majority electrons ($k = 1$) and holes ($k = 2$). For carriers which take part in the transition $(0^h - 0^e)_c$

$$\omega_{c3} = \frac{\Delta E(H)}{\hbar}, \quad n_3 = \frac{cH}{\pi^2 e\hbar}\Delta E \Big/ \frac{\partial E_3^0}{\partial k_z}, \quad \nu_3 \equiv \nu_{00}$$

are respectively analogs of the cyclotron frequency, the effective density, and the characteristic frequency which determines the momentum relaxation rate; $E_3^0 = 2\gamma_2 \cos(k_z c_0/2)$ is the energy of the degeneracy line of the valence band and conduction band for $H = 0$.

Equations (10) are obtained by neglecting the trigonal warping and the waves' spatial dispersion. For graphite $v_z^F \lesssim 2 \cdot 10^6$ cm/s; therefore even near the cyclotron resonances of the majority carriers we have the ratio $qv_z^F/|\omega - i\nu_j| \lesssim 0.03$ and the effect of spatial dispersion on $\sigma_{\alpha\beta}^{\omega}$ can be neglected. The trigonal warping leads not only to a change in the dispersion law of carriers for $H \lesssim 20$ kOe, but also to the appearance of harmonics of the cyclotron resonances of the majority carriers and to the appearance of singularities in the functions $\nu_k(H)$. However, the magnetic fields corresponding to resonance at the harmonics lie considerably below the fields of the fundamental resonances,

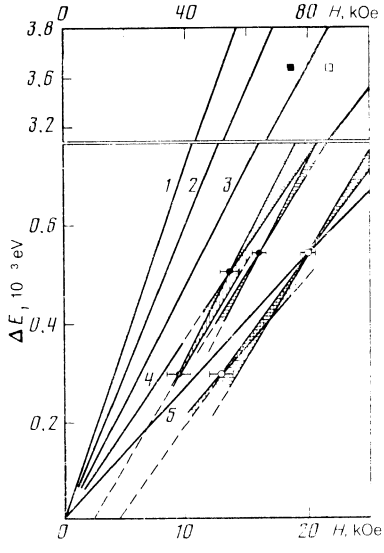

FIG. 5. Dependences of the energy ΔE of the transition $(0^e - 0^h)_c$ on magnetic field. Solid curves—calculation ($\gamma_3 = 0$, this paper); values of γ_6, meV: 25 (*1*); 0 (*2*); −25 (*3*); −50 (*4*); −75 (*5*). Points—experiment. Samples: ●—KG-1, ○—KG-2 (this paper); ■, □—HOPG from Ref. 35 (□—including the effect of coupled electron-hole plasma modes). We have hatched in the regions of possible values for the slope of the function $\Delta E(H)$.

and important changes in ν_k take place for $\omega_{ck}/\nu_k \lesssim 1$ ($k = 1,2$).[16] For $\omega_{ck} \gtrsim \omega \gtrsim \nu_k$ the contributions of the harmonics to $\sigma^{\omega}_{\alpha\beta}$ and the corrections to ν_k can be neglected, so that Eq. (10) is applicable for the case $\gamma_3 \neq 0$ by replacing the function $\Delta E(H)$ with $\Delta E(H - H_d)$ for $H > H_d$.

Expressions (10) lead to the following dispersion relation for the electron-active (upper branch) and hole-active waves (we can neglect the quantity $\varepsilon_L \approx 4$–9 (Ref. 37), since $\varepsilon_L \ll (4\pi/\omega)\sigma^{\omega}_{xx}$ for fields in the region of interest to us):

$$\left(q_j \frac{\omega}{c}\right)^2 = \pm \frac{4\pi ec}{\omega H} \sum_{k=1}^{3} n_k \left[\frac{\omega_{ck}}{(-1)^k \omega_{ck} \mp (\omega + i\nu_k)} + \delta_{k3} \right]. \tag{11}$$

We note that inclusion of interband transitions leads not only to the appearance of an additional resonance term $k = 3$ (i.e., to the cyclotron resonances of the majority carriers) in (11), but also to a weaker than $\propto H^{-1}$ dependence for $q(H)$ in the region of strong magnetic fields ($\omega_{ck} \gg \omega, \nu_k$; $k = 1$–3). In this region the contribution of the transition $(0^h - 0^e)_c$, in contrast to the contribution from the majority carriers (which is $\propto H^{-2}$), does not depend on H because $n_3 \propto H^2$.

The dispersion relation (11) together with (8) and (9) allows us to calculate the functions $M(1/H)$ and $\beta^*(H)$ for given values of the carrier parameters, and to compare these functions with experiments. For the values given in the table, the difference between the results of the calculation and the experimental results does not exceed the limits of experimental error (see Figs. 3 and 4) for $H \leqslant 20$ kOe.

The values of the parameters obtained here are in good agreement with the results of GM measurements[1] carried out on analogous samples, and also with the results of GM and HF measurements made by other authors.[2–5,7,8,22–25] An exception is the ratio $b = \mu_h/\mu_e$, whose value in the region of fields 3 kOe $\lesssim H \lesssim$ 15 kOe is considerably lower than the value $b = 1.05$–1.23 for $H \lesssim 1$ kOe.[1] The difference is due most likely to the actual dependence of b on the field.

The errors in determining the total carrier concentration[4)] $n_e + n_h$ and the absolute values of M are estimated (with a confidence coefficient of 0.9) on the basis of the value of the mean square of the discrepancy between the experimental and calculated functions $M(1/H)$. The maximum error (as $M \to 0$) of the absolute value of M (for $f = 131.9$ GHz) does not exceed ± 0.33 (sample KG-1), ± 0.30 (KG-2), and ± 0.22 (KG-3). The errors in the remaining parameters are determined by the ranges of the values of these parameters obtained from the various sets that describe satisfactorily the experimental curves. (Altogether, more than 500 different sets of parameters were analyzed with a computer for the three samples.)

By determining the absolute values of M with the help of the procedure described above and calibrating the absolute value of β^*, we were able to obtain the functions $D(H)$ and $\bar{\nu}(H)$. We note that the quasiclassical expressions used in Refs. 23 and 21 for D and $\bar{\nu}$ can hardly be correct in view of the complexity of the carrier energy spectrum and of the substantial contribution of interband transitions to the conductivity (especially in the region of a quantizing magnetic field). In connection with this it is advantageous to introduce the following definitions:

$$D(H) = \lim_{\omega/\omega_{ck},\, \nu_k/\omega_{ck} \to 0} \left[-\frac{H^2}{\omega c^2} \operatorname{Im} \sigma_{xx}^{\omega}(H) \right],$$
$$\bar{\nu}(H) = \lim_{\omega/\omega_{ck},\nu_k/\omega_{ck} \to 0} \left[-\omega \frac{\operatorname{Re} \sigma_{xx}^{\omega}}{\operatorname{Im} \sigma_{xx}^{\omega}} \right] \tag{12}$$

which generalize the concepts of mass density and average characteristic frequency for the carrier momentum relaxation rate for the case of strong quantization and/or the situation when contributions from interband transitions are important; these definitions are applicable to arbitrary carrier spectra. The quantities D and $\bar{\nu}$ defined in this way (in the absence of wave spatial dispersion) should not depend on the measurement frequency, and are characteristics of the material. This assertion is fully valid for $k_B T \gg \hbar\omega$; however, for the monotonic components of $\sigma^{\omega}_{\alpha\beta}$ (i.e., without allowance for the SdH oscillations) they are valid even when $T \to 0$. In the region of classical strong magnetic fields, and in the absence of interband transitions, Eq. (12) go over into the well-known classical expressions.

In Fig. 6 we show plots of $D(H)$ for the three samples. In weak fields ($H \lesssim 20$ kOe), $D = \text{const}$ (according to our calculations, as $H \to 0$ we have $D_{\text{theor}} = 1.88 \cdot 10^{-10}$ g/cm^3 and $n_e + n_h = 4.65 \cdot 10^{18}$ cm^{-3}), while for $H \gtrsim 20$ kOe we observe a rapid growth in D with field; in the region $30 \lesssim H \lesssim 60$ kOe, the increase in D is approximately linear, while for $H \gtrsim 60$ kOe it is superlinear. The functions $D(H)$ for the three samples are qualitatively similar and agree with the theoretical function (Fig. 6, curve 4) which follows from the results of quantum-mechanical calculations[5] of $\sigma^{\omega}_{\alpha\beta}$. Since D and Im σ^{ω}_{xx} are related through Eq. (12), measurement of the function $D(H)$ implies that the field dependences of Im σ^{ω}_{xx} and the conductivity $\sigma^{0}_{xx} \approx \rho_{xx}^{-1}$ are qualitatively similar at constant current in the region ($H \gtrsim 20$ kOe) of strong quantization and of the UQL, namely, for 20

TABLE I. Parameters for majority charge carriers in kish-graphite.

Sample	$n_e + n_h$, 10^{18} cm^{-3}	$\Delta n^{a)}$, 10^{18} cm^{-3}	m_h/m_0 [b)]	b
KG-1	3.78±0.22	0±0.02	0.039±0.001	0.4±0.1 (9–13) [c)]
KG-2	5.78±0.18	0±0.01	0.039±0.001	0.4±0.1 (9–15)
KG-3	2.50±0.25	0±0.02	0.045±0.001 [d)]	0.5±0.1 (3–4)

Notes. [a)] GM measurements carried out on one of the samples of this run imply that the deviation from complete carrier compensation was $\Delta n = -1.9 \cdot 10^{18}$ cm^{-3}. [b)] For the carrier masses we took the value at the extremal cross-section of their Fermi surface, i.e., $m_e = 0.057\, m_0$. [c)] The numbers in parentheses denote the region of magnetic fields (kOe) in which the value of b was determined. [d)] Determined near cyclotron resonance (3 kOe $\lesssim H \lesssim$ 4 kOe at $f = 131.9$ GHz and 1.5 kOe $\lesssim H \lesssim$ 2.5 kOe at $f = 71.5$ GHz), in which range the hole mass dispersion is substantial.

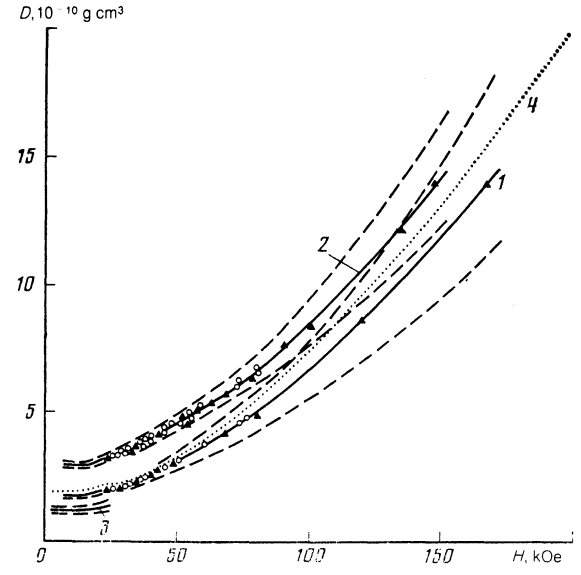

FIG. 6. Dependence of the carrier mass density D on magnetic field. *1–3*—experiment (magnetic field: ○—stationary, ▲—pulsed; for $H \leqslant 25$ kOe the points are not shown); *4*—calculation. Samples: *1*—KG-1; *2*—KG-2; *3*—KG-3. Shown by dashed lines are the limiting possible positions of curves *1–3*, connected with the accuracy of determination of the number of extrema.

kOe $\lesssim H \lesssim H_{\mathrm{UQL}}$ the values of Im σ_{xx}^{ω} and σ_{xx}^{0} decrease as H^{-1} with field, while for $H \gtrsim H_{\mathrm{UQL}}$ these values tend to constants.[29] At the same time, in classically strong and weakly-quantizing magnetic fields ($H \lesssim 20$ kOe) we have Im $\sigma_{xx}^{\omega} \propto H^{-2}$, whereas $\sigma_{xx}^{0} \propto H^{-1}$.

In this paper we have obtained the field dependences (Fig. 7) of the frequencies $\bar{\nu}$ and ν_{00} for the first time. The behavior of the function $\bar{\nu}(H)$ for $H \lesssim 20$ kOe differs qualitatively from its behavior for $H \gtrsim 20$ kOe; in the region of fields 3 kOe $\lesssim H \lesssim 20$ kOe the frequency increases approximately linearly with field, while for $H \gtrsim 20$ kOe it either remains approximately constant for 20 kOe $\lesssim H \lesssim H_{\mathrm{UQL}} \approx 70$ kOe [if we do not consider the SdH oscillations, which are connected not so much with oscillations in the momentum relaxation rate as with the method of averaging of (12)], or falls off as H increases (for $H \gtrsim H_{\mathrm{UQL}}$). We note that the difference in the temperature dependences of ρ_{xx} in these regions of H (Refs. 16 and 17) also indicate qualitative differences in the character of the scattering of carriers.

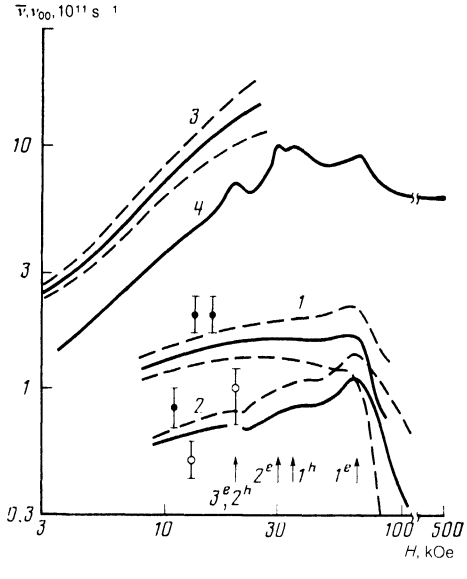

FIG. 7. Dependence of the frequencies $\bar{\nu}$ (solid curves) and ν_{00} (points) on magnetic field: *1–3*—HF measurements. Samples: *1*, ●—KG-1; *2*, ○—KG-2; *3*—KG-3. Shown with dashed lines are the limiting possible positions of curves *1–3*, connected with the accuracy of determining the absolute magnitude of wave attenuation in the sample. Curve *4* was obtained according to the results of GM measurements[1] (sample nos. *3–5*) and calculations of $D(H)$. We mark with arrows the fields at which the Landau levels coincide with the Fermi level.

The function $\bar{\nu}(H)$ obtained from HF measurements agrees with the function (Fig. 7, curve 4) $\bar{\nu} = H^2\sigma_{xx}/c^2 D_{\mathrm{theor}}$ obtained from the results of GM measurement[1] and calculations of $D(H)$. An exception is the UQL region, where the jump in $\bar{\nu}$ which appears in the GM measurements[1] is significantly smaller. The disagreement could be caused by errors (underestimates) in the value of the AW attenuation in the samples, or could be related to smaller momentum relaxation rates in samples KG-1 and KG-2 (i.e., smaller than in samples Nos. 3–5 from Ref. 1). According to the GM measurements of Refs. 14–15, for samples with small momentum relaxation rates and for $T \lesssim 4.2$ K a jump in $\rho_{xx}(H)$ was observed in passing to the UQL, which is smoothed out in samples with larger momentum relaxation rates and with increase of T.[1,15–18] An analogous jump should also be observed in the function Re $\sigma_{xx}^{\omega}(H)$, which according to (12) will appear as a jump in $\bar{\nu}$ in passing to the UQL.

CONCLUSION

The results of this paper allow us to resolve the contradiction between the results of GM measurements[1–20] and earlier investigations[22–25] of the propagation of AW in graphite. The origin of this contradiction is the incorrect treatment in Refs. 22–25 of the results of interference measurements, and is connected with the use of the semimetal model with carrier parameters n_j, m_j and ν_j which were field-independent, without sufficient basis for such an interpretation of the data.

The dependences of D and $\bar{\nu}$ on magnetic field measured in this paper, and the proposed connection of the linear growth (for $H \gtrsim 20$ kOe) and saturation of the function $\rho_{xx}(H)$ with the growth of the mass density of the carriers, allows us to make a unique choice between two alternative approaches to the interpretation of the function $\rho_{xx}(H)$ of graphite; moreover, it shows that the causes of the peculiarities in the latter must be sought in the singularities of the band structure of graphite. Thus, the interpretation in Refs. 13 and 17 of the linear growth and saturation of $\rho_{xx}(H)$ in the UQL as being the result of a complicated field dependence of the momentum relaxation rate is not confirmed. The reason is apparently the use of the Thomas-Fermi approximation by the authors of Refs. 13–17 in their calculations of the screening of impurity centers,[38] which also leads to a strong dependence of $\nu_j(H)$ which is not observed in experiment. On the contrary, according to data from the HF measurements, a significant dependence $\bar{\nu}(H) \propto H$ occurs in the region of weakly-quantizing and classically strong fields ($H \lesssim 20$ kOe), and it is this which explains the singularities in the function $\rho_{xx}(H)$ for $H \lesssim 20$ kOe.

Thus, this paper, having answered two questions—what is the cause of the discrepancy between the results of GM and HF measurements, and what is the effect of singularities in the carrier scattering and band structure on the anomalous character of the function $\rho_{xx}(H)$ for graphite—raises two new questions: what is the cause of the linear growth of the momentum relaxation rate for carriers for $H \lesssim 20$ kOe, and what is the cause of the rapid growth in the carrier mass density for $H \lesssim 20$ kOe. In particular, the superlinear growth of $D(H)$ in the UQL cannot be explained by the increase in carrier concentration with magnetic field, because according to Ref. 27 the linear growth in $n(H)$ takes place in fields 30 kOe $\lesssim H \lesssim$ 400 kOe, and cannot lead to the appearance of a superlinear dependence of $D(H)$ for $H \gtrsim 60$ kOe. The efforts of the authors of Ref. 31 to relate the superlinear growth of D to nonparabolicity in the energy spectrum of graphite, and consequently to the rise in effective mass of the carriers with field, hardly merits serious discussion; although this effect also can lead to a superlinear dependence in $D(H)$, the magnitude of the corresponding correction is insufficient to explain the experimental $D(H)$ dependence, not to mention the fact that use of the quasiclassical concept of effective mass can hardly be correct in the UQL.

An explanation of the connection between the peculiarities in the field dependences of D and ρ_{xx} and the band structure of graphite requires a calculation of the HF conductivity of the latter over a wide range of magnetic fields; this calculation should be based on sufficiently general expressions for the conductivity and should include to the maximum extent possible the details of the graphite band structure. The field dependence of the HF conductivity of graphite must be compared with the results of GM and HF measurements. Preliminary calculations show that an adequate description of experiment based on the SW model is possible, starting only with a representation of the graphite band structure as a superposition of the band structures of a semimetal and a two-dimensional zero-gap semiconductor, and assigning a decisive role to interband transitions.

[1)] An analogous situation arises when a Fabry-Perot interferometer is used.[31] The error in determining the absolute number of extrema because the quasiclassical dispersion law is used for AW in quantizing magnetic fields and in the UQL also apparently leads to the overestimate in Ref. 31 of the mass density of carriers compared to the results of our measurements.

[2)] The direction of rotation of the plane of polarization of these waves coincides (for a given direction of H) with the direction of rotation of the corresponding electrons and holes.

[3)] In Figs. 3 and 4 the experimental points for the direction H^- of the magnetic field are only partially plotted, in particular only for those regions of H where the difference in the positions and amplitudes of the interference extrema is significant for the two directions of H.

[4)] $n_c + n_h$ is determined accurate to a coefficient $(1 \pm \delta l/l)^2$ connected with the error $\delta l = 2\mu$ in the measured thickness of the sample.

[5)] The difference between the values of $D(H \to 0)$ and $n_c + n_h$ (see the table), which significantly exceed the experimental errors, can be explained by the presence in the sample of a "distorted" phase in which the overlap of the valence and conduction bands is different from the band overlap in an ideal graphite lattice.

[1]H. B. Brandt, G. A. Kapustin, V. G. Karavaev *et al.*, Zh. Eksp. Teor. Fiz. **67**, 1138 (1974) [Sov. Phys. JETP **40**, 564 (1975)].
[2]D. E. Soule, Phys. Rev. **112**, 698 (1958).
[3]L. C. Blackman, G. A. Saunders, and A. R. Ubbelohde, Proc. Roy. Soc. London A **264**, 19 (1961).
[4]I. L. Spain, A. R. Ubbelohde, and D. A. Young, Phil. Trans. Proc. Roy. Soc. London A **262**, 345 (1967).
[5]Y. Hishiyama, A. Ono, T. Tsuzuku, and T. Takezawa, Jpn. J. Appl. Phys. **11**, 958 (1972).
[6]K. Kawamura, T. Saito, and T. Tsuzuku, J. Phys. Soc. Jpn. **42**, 574 (1977).
[7]R. O. Dillon, I. L. Spain, J. A. Woollam, and W. H. Lowrey, J. Phys. Chem. Solids **39**, 1978 (1978).
[8]C. Ayache, Physica **B99**, 509 (1980).
[9]D. E. Soule, Phys. Rev. **112**, 708 (1958).
[10]D. E. Soule, J. W. McClure, and L. B. Smith, Phys. Rev. **134**, A453 (1964).
[11]J. A. Woollam, Phys. Rev. Lett. **25**, 810 (1970).
[12]J. A. Woollam, Phys. Rev. **B4**, 1148 (1971).
[13]J. W. McClure and W. J. Spry, Phys. Rev. **165**, 809 (1968).
[14]J. A. Woollam, Phys. Lett. **A32**, 371 (1970).
[15]J. A. Woollam, D. J. Sellmeyer, R. O. Dillon, and I. L. Spain, *Low Temperature Physics–LT13* (New York, London, 1974), Vol. 4 (Plenum Press, New York, 1975), p. 358.
[16]L. W. Kreps and J. A. Woollam, Carbon **15**, 403 (1977).
[17]K. Sugihara and J. A. Woollam, J. Phys. Soc. Jpn. **45**, 1891 (1978).
[18]W. H. Lowrey and I. L. Spain, Solid State Commun. **22**, 615 (1977).
[19]S. Tanuma, Y. Onuki, R. Inada *et al.*, *Physics in High Magnetic Fields*, edited by S. Chikazumi and N. Miura (Springer-Verlag, Berlin, 1981), p. 316.
[20]Y. Iye and G. Dresselhaus, Phys. Rev. Lett. **54**, 1182 (1958).
[21]J. G. Slonczewski and P. R. Weiss, Phys. Rev. **109**, 272 (1958).
[22]M. Surma, J. K. Furdyna, and H. C. Praddaude, Phys. Rev. Lett. **13**, 710 (1964).
[23]A. R. Krauss and J. K. Furdyna, *Proceedings of the Conference on the Physics of Semimetals and Narrow-Gap Semiconductors* (Dallas, Texas, 1970, edited by D. L. Carter and R. T. Bate; London; Pergamon Press, 1971), p. 165.
[24]A. R. Krauss and J. K. Furdyna, Phys. Rev. **B7**, 2520 (1973).
[25]G. Alquié and A. Kreisler, Phys. Status Solidi **A29**, 77 (1975).
[26]K. Sugihara and S. Ono, J. Phys. Soc. Jpn. **21**, 631 (1966).
[27]G. A. Kapustin and E. Z. Meilikhov, Fiz. Tverd. Tela (Leningrad) **17**, 2978 (1975) [Sov. Phys. Solid State **17**, 1979 (1975)].
[28]E. D. Palik and J. K. Furdyna, Rep. Prog. Phys. **33**, 1193 (1970).
[29]G. A. Kapustin, A. S. Kotosonov, and E. Z. Meĭlikhov, Abstracts from the 3rd Symposium on Plasma and Instabilities in Semiconductors (Vilnius, 1977; Vilnius: Izd, IFP, Lithuanian SSR Acad. Sci., 1977), p. 66.
[30]G. A. Kapustin, V. S. Babichenko, and E. Z. Meilikhov, Solid State Commun. **52**, 913 (1984).
[31]K. Nakamura and N. Miura, Solid State Commun. **42**, 119 (1982).
[32]K. Nakao, J. Phys. Soc. Jpn. **40**, 761 (1976).
[33]O. R. Gupta and P. R. Wallace, Phys. Status Solidi **B54**, 53 (1972).
[34]H. Nagayoshi, K. Nakao, and Y. Uemura, J. Phys. Soc. Jpn. **41**, 1480 (1976).
[35]K. Nakamura, G. Kido, K. Nakao, and N. Miura, J. Phys. Soc. Jpn. **53**, 1164 (1984).
[36]R. O. Dillon and I. L. Spain, J. Phys. Chem. Solids **39**, 923 (1978).
[37]E. A. Taft and H. R. Philipp, Phys. Rev. **138**, A197 (1965).
[38]G. A. Kapustin, A. S. Lagutin, and E. Z. Meilikhov, Fiz. Tverd. Tela (Leningrad) **23**, 3273 (1981) [Sov. Phys. Solid State **23**, 1902 (1981)].

Translated by F. Crowne